

# <sup>18</sup>F-MCL-524, an <sup>18</sup>F-Labeled Dopamine D<sub>2</sub> and D<sub>3</sub> Receptor Agonist Sensitive to Dopamine: A Preliminary PET Study

Sjoerd J. Finnema<sup>\*1</sup>, Vladimir Stepanov<sup>\*1</sup>, Ryuji Nakao<sup>1</sup>, Anna W. Sromek<sup>2</sup>, Tangzhi Zhang<sup>2</sup>, John L. Neumeyer<sup>2</sup>, Susan R. George<sup>3</sup>, Philip Seeman<sup>3</sup>, Michael G. Stabin<sup>4</sup>, Cathrine Jonsson<sup>5</sup>, Lars Farde<sup>1,6</sup>, and Christer Halldin<sup>1</sup>

<sup>1</sup>Karolinska Institutet, Department of Clinical Neuroscience, Center for Psychiatric Research, Stockholm, Sweden; <sup>2</sup>McLean Hospital, Harvard Medical School, Belmont, Massachusetts; <sup>3</sup>University of Toronto, Toronto, Ontario, Canada; <sup>4</sup>Department of Radiology and Radiological Sciences, Vanderbilt University, Nashville, Tennessee; <sup>5</sup>Department of Nuclear Medicine, Karolinska University Hospital, Stockholm, Sweden; and <sup>6</sup>AstraZeneca, Translational Science Center at Karolinska Institutet, Stockholm, Sweden

PET has been used to examine changes in neurotransmitter concentrations in the living brain. Pioneering PET studies on the dopamine system have used D<sub>2</sub> and D<sub>3</sub> receptor (D<sub>2</sub>/D<sub>3</sub>) antagonists such as <sup>11</sup>C-raclopride. However, more recently developed agonist radioligands have shown enhanced sensitivity to endogenous dopamine. A limitation of available agonist radioligands is that they incorporate the short-lived radioisotope <sup>11</sup>C. In the current study, we developed the <sup>18</sup>F-labeled D<sub>2</sub>/D<sub>3</sub> receptor agonist (R)-(-)-2-<sup>18</sup>F-fluoroethoxy-N-*n*-propylnorapomorphine (<sup>18</sup>F-MCL-524). **Methods:** In total, 10 PET measurements were conducted on 5 cynomolgus monkeys. Initially, the binding of <sup>18</sup>F-MCL-524 was compared with that of <sup>11</sup>C-MNPA in 3 monkeys. Second, the specificity of <sup>18</sup>F-MCL-524 binding was examined in pretreatment studies using raclopride (1.0 mg/kg) and D-amphetamine (1.0 mg/kg). Third, a preliminary kinetic analysis was performed using the radiometabolite-corrected arterial input function of the baseline studies. Finally, 2 whole-body PET measurements were conducted to evaluate biodistribution and radiation dosimetry after intravenous injection of <sup>18</sup>F-MCL-524. **Results:** <sup>18</sup>F-MCL-524 entered the brain and provided striatum-to-cerebellum ratios suitable for reliable quantification of receptor binding using the multilinear reference tissue model. Mean striatal nondisplaceable binding potential (BP<sub>ND</sub>) values were 2.0 after injection of <sup>18</sup>F-MCL-524 and 1.4 after <sup>11</sup>C-MNPA. The ratio of the BP<sub>ND</sub> values of <sup>18</sup>F-MCL-524 and <sup>11</sup>C-MNPA was 1.5 across striatal subregions. After administration of raclopride and D-amphetamine, the <sup>18</sup>F-MCL-524 BP<sub>ND</sub> values were reduced by 89% and 56%, respectively. Preliminary kinetic analysis demonstrated that BP<sub>ND</sub> values obtained with the 1-tissue- and 2-tissue-compartment models were similar to values obtained with the multilinear reference tissue model. Estimated radiation doses were highest for gallbladder (0.27 mSv/MBq), upper large intestine (0.19 mSv/MBq), and small intestine (0.17 mSv/MBq). The estimated effective dose was 0.035 mSv/MBq. **Conclusion:** The <sup>18</sup>F-labeled agonist <sup>18</sup>F-MCL-524 appears suitable for quantification of D<sub>2</sub>/D<sub>3</sub> receptor binding in vivo, and the results encourage extension to human studies. The longer half-life of <sup>18</sup>F makes <sup>18</sup>F-MCL-524 attractive for studies on modulation of the dopamine concentration—for example, in combination with simultaneous measurement of changes in blood-oxygen-level-dependent signal using bimodal PET/functional MRI.

**Key Words:** <sup>18</sup>F-MCL-524; agonist; dopamine; monkey; PET

**J Nucl Med** 2014; 55:1164–1170

DOI: 10.2967/jnumed.113.133876

Classic receptor-binding assays have demonstrated that dopamine receptors exist in 2 affinity states for agonists (1), similar to other G protein-coupled receptors. The 2 affinity states are considered interconvertible, with the high-affinity state corresponding to the functional, G protein-coupled state of the receptor (2). PET studies of dopamine D<sub>2</sub> and D<sub>3</sub> receptors (D<sub>2</sub>/D<sub>3</sub>) have since long predominantly been conducted using antagonists, such as <sup>11</sup>C-raclopride. However, antagonists bind with equal affinity to the 2 affinity states of the receptor and do not provide information on the fraction of receptors in the high-affinity state. To overcome this limitation, agonist radioligands have more recently been developed (3), including <sup>11</sup>C-N-propylnorapomorphine (<sup>11</sup>C-NPA) (4), <sup>11</sup>C-MNPA (5), and <sup>11</sup>C-4-propyl-9-hydroxynaphthoxazine (6). A reported advantage of these agonist radioligands is the enhanced sensitivity to amphetamine-induced changes in dopamine concentration when compared with <sup>11</sup>C-raclopride (7,8).

A limitation of the currently available agonist radioligands is the labeling with the relatively short-lived radioisotope <sup>11</sup>C (half-life, 20.3 min). Radiolabeling of an agonist with a longer-lived radioisotope, such as <sup>18</sup>F (half-life, 109.8 min), may provide several advantages. First, an <sup>18</sup>F-labeled ligand may favorably be used with bolus-infusion techniques, which allow quantification of binding potential at baseline and at a series of dopamine concentration-altering conditions in a single PET measurement. This paradigm is particularly attractive for application in the recently developed PET/functional MRI systems that allow for simultaneous measurements of changes in neurotransmitter concentration and blood-oxygen-level-dependent signal (9). Second, the longer half-life of <sup>18</sup>F will allow for studies evaluating the acute and prolonged effects of a dopamine-related change in receptor binding, thereby having potential to disentangle return of dopamine levels to baseline from receptor internalization (10). Third, the longer half-life of <sup>18</sup>F enhances the feasibility of radioligands to be used in clinical centers where no cyclotron is available for on-site radioligand production. An <sup>18</sup>F-labeled radioligand with high sensitivity to the endogenous dopamine concentration may therefore have wide utility.

Received Dec. 3, 2013; revision accepted Mar. 17, 2014.

For correspondence or reprints contact: Sjoerd J. Finnema, Karolinska Institutet, Department of Clinical Neuroscience, Center for Psychiatric Research, Karolinska University Hospital, Building R5:02, SE-17176 Stockholm, Sweden.

E-mail: [sjoerd.finnema@ki.se](mailto:sjoerd.finnema@ki.se)

\*Contributed equally to this work.

Published online May 1, 2014.

COPYRIGHT © 2014 by the Society of Nuclear Medicine and Molecular Imaging, Inc.

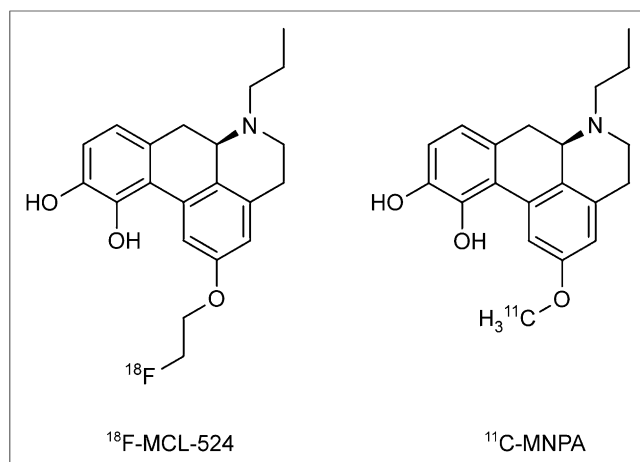


**FIGURE 1.** Chemical structures of  $^{18}\text{F}$ -MCL-524 and  $^{11}\text{C}$ -MNPA.

Development of  $^{18}\text{F}$ -labeled  $\text{D}_2/\text{D}_3$  receptor agonist radioligands has previously been reported, but with only limited success (11).  $^{18}\text{F}$ -analogs of successful  $^{11}\text{C}$ -labeled aporphine and naphthoxazine scaffold-based radioligands have not been promising (12,13), because the introduction of  $^{18}\text{F}$  into the  $N$ -alkyl chain decreases binding affinity significantly. Perhaps the most promising radioligand so far is (*R,S*)-2-(*N*-propyl-*N*-(5'- $^{18}\text{F}$ -fluoropentyl)amino)-5-hydroxytetralin, though the reported striatal-to-cerebellum binding ratios were only 2.0 in monkeys (14). Follow-up studies with this radioligand have so far not been reported.

In the current study, we radiolabeled the aporphine (*R*)-(-)-2- $^{18}\text{F}$ -fluoroethoxy-*N*-*n*-propylnorapomorphine ( $^{18}\text{F}$ -MCL-524) (Fig. 1). This compound has nanomolar affinity in vitro to the  $\text{D}_2$  receptor in a state of high affinity ( $\text{D}_2^{\text{high}}$ ) (3.7 nM) (15), and the radionuclide can be remotely introduced into the substituent at the 2-position. After radiosynthesis,  $^{18}\text{F}$ -MCL-524 was evaluated by PET in cynomolgus monkeys. We compared the binding of  $^{18}\text{F}$ -MCL-524 to  $^{11}\text{C}$ -MNPA and conducted pretreatment studies with raclopride and *D*-amphetamine to confirm specific binding to the  $\text{D}_2/\text{D}_3$  receptors and dopamine sensitivity. A preliminary kinetic analysis was performed using the radiometabolite-corrected arterial input function. Finally, 2 whole-body PET examinations were conducted to obtain dosimetry estimates in preparation for future human studies.

## MATERIALS AND METHODS

### Preparation of Radioligands

The standard MCL-524 was prepared according to previously reported methods (15). The synthesis of the corresponding tosylated precursor

MCL-556 is described in the supplemental information (supplemental materials are available at <http://jnm.snmjournals.org>). All other chemicals and materials were obtained from commercial sources, were of analytic grade, and were used as received.  $^{18}\text{F}$ -MCL-524 was prepared in 2 steps. Direct fluorination of MCL-556 was followed by deprotection of the catechol moiety (supplemental information).  $^{11}\text{C}$ -MNPA was prepared using previously described procedures (16).

### PET Studies on Nonhuman Primates

The study was approved by the Animal Research Ethical Committee of the Northern Stockholm region (diarienummer N386/09, N399/08, and N452/11) and was performed according to local (diarienummer 4820/06-600) and international guidelines (17). Five cynomolgus monkeys (*Macaca fascicularis*) (M1–M5), weighing 4–8 kg, were included in the study. Anesthesia and experimental procedures were similar to those reported before (18). PET measurements of the brain or whole body were conducted using a high-resolution research tomograph (HRRT; Siemens Molecular Imaging) or the Biograph TruePoint TrueV PET/CT system (Siemens Medical Solutions), respectively, and followed previously reported procedures (18–20).

**PET Studies Using HRRT.** On each of 3 experimental days, baseline PET measurements after injection of  $^{18}\text{F}$ -MCL-524 and  $^{11}\text{C}$ -MNPA were performed to allow for a direct comparison of the 2 radioligands. PET measurements with  $^{11}\text{C}$ -MNPA were conducted 2.5 h before injection of  $^{18}\text{F}$ -MCL-524 in 3 cynomolgus monkeys (M1–M3).

To characterize the specificity and dopamine sensitivity of  $^{18}\text{F}$ -MCL-524 receptor binding, pretreatment studies were performed using the  $\text{D}_2/\text{D}_3$  receptor antagonist raclopride (in M1) and the dopamine-releasing drug *D*-amphetamine (in M2), respectively. The pretreatment studies were performed on monkeys (M1 and M2) for which baseline data had been obtained at least 1 mo earlier as described above. Raclopride (1.0 mg/kg, tartrate salt, in phosphate-buffered saline) was infused intravenously over 10 min, starting 23 min before the injection of  $^{18}\text{F}$ -MCL-524. *D*-amphetamine (1.0 mg/kg, sulfate salt, in phosphate-buffered saline) was infused intravenously over 15 min, starting 29 min before the injection of  $^{18}\text{F}$ -MCL-524.

To allow for a preliminary assessment of the quantification methods suitable for  $^{18}\text{F}$ -MCL-524, arterial blood sampling was included in the 3 baseline PET studies described above. A cannula was inserted in the femoral artery or an artery of the lower limb, and arterial blood was collected continuously for 3 min using an automated blood sampling system (Allogg AB) at a speed of 3.0 mL/min. Blood samples (1.0–3.0 mL) were drawn at 0.5, 1.0, 1.5, 2.0, 3.0, 6.0, and 8.0 min for blood and plasma radioactivity and at 2.5, 5.0, 15, 30, 45, 60, 90, and 120 min for metabolite correction. One blood sample was taken before radioligand injection for determination of radioligand binding to plasma proteins.

Unchanged radioligand and radiometabolite fractions in plasma were determined using a previously described reversed-phase high-performance liquid chromatography method (18). The mobile phase system consisted of acetonitrile (A) and phosphoric acid (0.01 M) (B) eluted at 6.0 mL/min, according to the following program: 0–7 min (A/B), 15/85 → 40/60 v/v; 7–9 min (A/B), 40/60 v/v; 9–9.5 min (A/B), 15/85 v/v; 9.5–12 min (A/B), 15/85 v/v. The free fraction,  $f_p$ , in plasma was estimated using a previously reported ultrafiltration method (18).

**PET Studies Using PET/CT.** For determination of biodistribution and radiation dosimetry, 2 different cynomolgus monkeys (M4 and M5) were evaluated according to previously reported procedures (19) using the Biograph PET/CT system after intravenous injection of  $^{18}\text{F}$ -MCL-524.

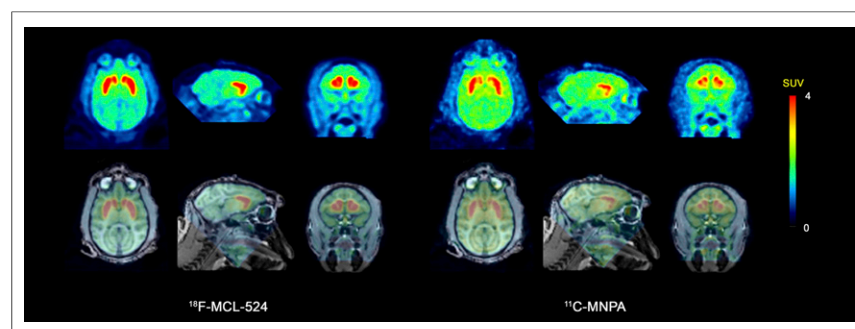


**FIGURE 2.** PET (mean, 9–123 min) and fused PET/MR images for  $^{18}\text{F}$ -MCL-524 and  $^{11}\text{C}$ -MNPA. SUV = standardized uptake value.

**TABLE 1**  
 **$BP_{ND}$  Values of  $^{18}\text{F}$ -MCL-524 and  $^{11}\text{C}$ -MNPA**

Region	$^{18}\text{F}$ -MCL-524				$^{11}\text{C}$ -MNPA				$^{18}\text{F}$ -MCL-524/ $^{11}\text{C}$ -MNPA			
	M1	M2	M3	Mean	M1	M2	M3	Mean	M1	M2	M3	Mean
Striatum	2.3	2.1	1.7	2.0	1.2	1.5	1.4	1.4	1.9	1.3	1.2	1.5
Putamen	2.4	2.2	1.7	2.1	1.3	1.7	1.3	1.4	1.8	1.3	1.3	1.5
Caudate nucleus	2.1	1.9	1.8	2.0	1.1	1.4	1.5	1.4	1.9	1.3	1.2	1.5
Ventral striatum	1.6	1.5	1.4	1.5	0.8	1.1	1.2	1.0	2.0	1.4	1.2	1.5

### Image Analysis and Quantification

All image analyses and PET quantification were performed using PMOD (version 3.308; PMOD Technologies Ltd.).

**PET Studies Using HRRT.** An average PET image (mean of 0–12 min) was automatically coregistered to an MR image. Volumes of interest were delineated on the individual template MR images for the caudate nucleus, cerebellum, midbrain, putamen, thalamus, ventral striatum, and whole brain. The volume of interest for the cerebellum included only cerebellar hemispheres. The striatum was defined as the volume-weighted mean of the striatal subregions. Decay-corrected time–activity curves for all regions were plotted over time, and radioactivity concentrations were expressed as the standardized uptake value ( $\text{g}\cdot\text{cm}^{-3}$ ).

Regional nondisplaceable binding potential ( $BP_{ND}$ ) values were calculated with the multilinear reference tissue model (MRTM) (equilibrium time, 0 min) using the cerebellum as the reference region (21). In the preliminary kinetic analysis, the time–activity curves were interpreted using the 1-tissue-compartment model (1TCM) and the 2-tissue-compartment model (2TCM). Graphical analysis (GA) was performed by using the Logan plot and with an equilibrium time of 21 min (22). The outcome parameters were the total distribution volume ( $V_T$ ) and the  $BP_{ND}$  obtained using the cerebellum as the reference region (23).  $BP_{ND}$  values were also calculated for the tissue compartment models and GA as (striatal  $V_T$ /cerebellum  $V_T - 1$ ) and compared with the  $BP_{ND}$  values obtained with the MRTM (21).

The radiometabolite-corrected plasma concentration of  $^{18}\text{F}$ -MCL-524 was used as the input function. The relative blood volume in brain was defined as 0.05. The Akaike information criterion and  $F$  statistics of the sum of squared residuals were used to compare the fits of the 1TCM and 2TCM analyses. The identifiability of the kinetic parameters was assessed using the SE coefficients of variation. To assess the time stability of  $V_T$  and  $BP_{ND}$  values, the effect of the duration of the PET measurement was evaluated by truncating the PET datasets from 120 to 30 min.

**PET Studies Using PET/CT.** Volumes of interest were defined for the brain, parotid glands, thyroid gland, lungs, heart, liver, gallbladder, upper gastrointestinal tract (stomach and duodenum), lower gastrointestinal tract, spleen, kidneys, bladder, and bone (claviculae) using CT. The remainder was estimated by drawing a large volume of interest around the whole body and by subtracting the radioactivity measured in the individual organs. The regional radioactivity concentration in each of the 2 whole-body PET measurements was decay-corrected to the time of injection and expressed as percentage injected radioactivity and plotted versus time. Estimates of the absorbed radiation dose in humans were calculated using the OLINDA/EXM software. Percentages of injected radioactivity per organ were fitted using the SAAM II software (24). Time integrals of activity (25) were then entered into the OLINDA/EXM software (26), using the adult male model. Activity was observed in the intestines and urinary bladder. Data for the bladder were fit to a retention function, as was done for the other organs. The number of disintegrations in the remainder of the body was assumed to be equal to 100% of the activity administered integrated to total decay of  $^{18}\text{F}$ , minus the disintegrations in other organs.

### RESULTS

#### Preparation of Radioligands

$^{18}\text{F}$ -MCL-524 was obtained with a mean specific radioactivity of 226 GBq/ $\mu\text{mol}$  (range, 125–568 GBq/ $\mu\text{mol}$ ) at the time of injection, corresponding to an injected mass of 0.34  $\mu\text{g}$  (range, 0.10–0.47  $\mu\text{g}$ ).  $^{18}\text{F}$ -MCL-524 was found to be stable for at least 2 h in the formulation prepared for injection.  $^{11}\text{C}$ -MNPA was obtained with a specific radioactivity of more than 185 GBq/ $\mu\text{mol}$ , corresponding to an injected mass of less than 0.26  $\mu\text{g}$ . The radiochemical purity for the injected radioligands was typically greater than 95%.

#### Comparison with $^{11}\text{C}$ -MNPA and Pretreatment Studies

After injection of  $^{18}\text{F}$ -MCL-524, the radioactivity concentration was higher in the striatum and lower in the cerebellum than for  $^{11}\text{C}$ -MNPA (Fig. 2). The mean striatal  $BP_{ND}$  values were 2.0 after injection of  $^{18}\text{F}$ -MCL-524 and 1.4 after  $^{11}\text{C}$ -MNPA. The ratio of the  $BP_{ND}$  values of  $^{18}\text{F}$ -MCL-524 and  $^{11}\text{C}$ -MNPA was 1.5 across striatal subregions (Table 1).

$^{18}\text{F}$ -MCL-524 binding in the striatum, but not in the cerebellum, decreased after administration of raclopride (1.0 mg/kg) or D-amphetamine (1.0 mg/kg) (Fig. 3). After administration of raclopride, the striatal  $BP_{ND}$  was 0.25, which corresponds to an 89% reduction from baseline conditions. After D-amphetamine, the striatal  $BP_{ND}$  decreased to 0.92, which corresponds to a 56% reduction from baseline conditions.

#### Radiometabolite Analyses and Preliminary Kinetic Analysis

A representative high-performance liquid radiochromatogram, obtained at 60 min after injection of  $^{18}\text{F}$ -MCL-524, is displayed in Figure 4A. After injection of  $^{18}\text{F}$ -MCL-524, several radiometabolite fractions could be measured during the time course of the PET measurement. All observed radiometabolite fractions had a retention time shorter than  $^{18}\text{F}$ -MCL-524 (8.8 min).  $^{18}\text{F}$ -MCL-524 was

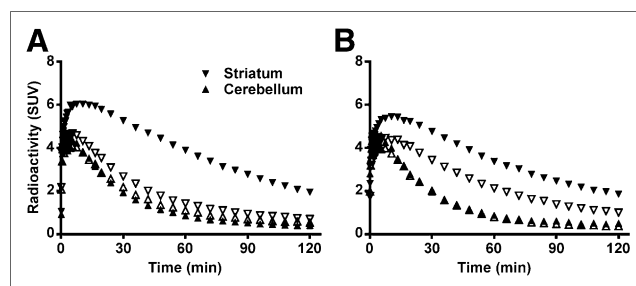


**FIGURE 3.** Time–activity course after injection of  $^{18}\text{F}$ -MCL-524 at baseline, after raclopride (A), and after D-amphetamine (B). Closed symbols represent baseline and open symbols pretreatment condition. SUV = standardized uptake value.

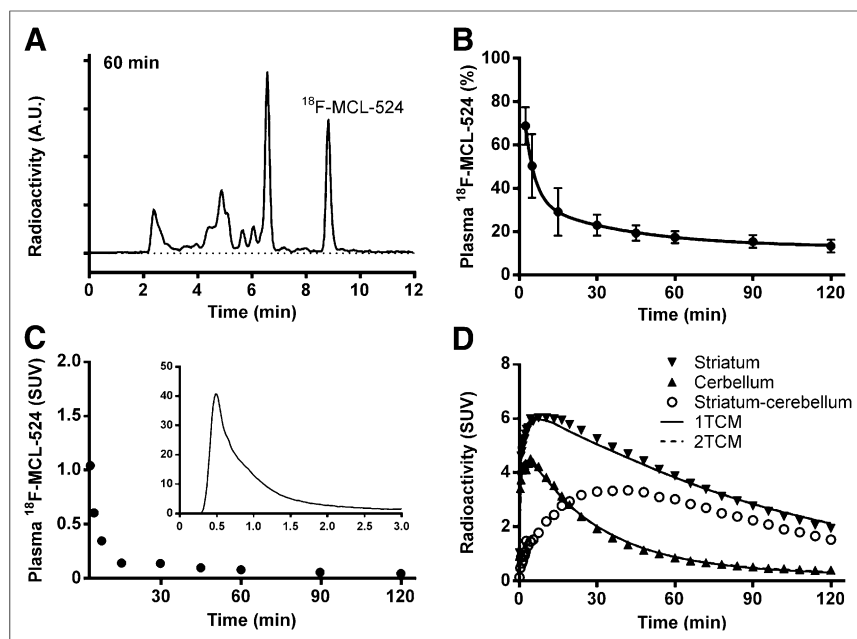


**FIGURE 4.** High-performance liquid radiochromatogram (A), plasma  $^{18}\text{F}$ -MCL-524 fraction (B), radiometabolite-corrected arterial input function (C), and time-activity course with 1TCM and 2TCM fit (D). A.U. = arbitrary units; SUV = standardized uptake value.

rapidly metabolized, and mean unchanged radioligand accounted for 50% of the plasma radioactivity at 5 min and 13% at 120 min after injection (Fig. 4B). The mean  $f_p$  was 0.07 for  $^{18}\text{F}$ -MCL-524 and 0.10 for  $^{11}\text{C}$ -MNPA at baseline conditions.

After injection of  $^{18}\text{F}$ -MCL-524, the radioactivity in plasma representing unchanged radioligand decreased rapidly (Fig. 4C). The time-radioactivity curves for the cerebellum and striatum could be described with the 1TCM as well as the 2TCM (Fig. 4D). The 1TCM was the preferred model for the striatum and cerebellum in all 3 monkeys, according to  $F$  statistics of the sum of squared residuals ( $P < 0.05$ ) and a lower Akaike information criterion (Table 2; Fig. 4D). Both models provided reliable estimates of  $V_T$  values, except for the 2TCM analysis of the cerebellum in one monkey. Individual rate constants could be reliably identified only with the 1TCM (Table 2). Mean  $V_T$  values calculated by using the rate constants obtained from the 1TCM were  $16.5 \text{ mL}\cdot\text{cm}^{-3}$  for the striatum and  $5.0 \text{ mL}\cdot\text{cm}^{-3}$  for the cerebel-

lum and similar when calculated with rate constants from the 2TCM (Table 2). Mean striatal  $V_T$  values were 7% lower when calculated with GA than when calculated with the 1TCM (Table 2). Mean striatal  $BP_{ND}$  values calculated with the 1TCM and GA were 2.3 and 2.1, respectively, compared with 2.0 obtained with the MRTM (Table 3).  $BP_{ND}$  values were reliably calculated with a PET duration of 60 min for the MRTM and 90 min for the 1TCM.

## Whole-Body Distribution and Radiation Dosimetry

The uptake of radioactivity (percentage injected radioactivity) was highest in the lungs (20% at  $\sim 1$  min), kidneys (9% at  $\sim 1$  min), and liver (9% at  $\sim 9$  min) and lower in the heart (2% at  $\sim 1$  min) and bone (2% at  $\sim 1$  min) (Figs. 5 and 6).  $^{18}\text{F}$ -MCL-524 was eliminated mainly through the intestine, with the highest accumulation occurring at about 228 min in the upper gastrointestinal tract (31%), lower gastrointestinal tract (15%), gallbladder (7%), and urinary bladder (8%). Extrapolation to human dose estimates found

that the largest absorbed dose was to the gallbladder, followed by the upper large intestine and small intestine. The average calculated effective dose was  $0.035 \text{ mSv/MBq}$  (Table 4).

## DISCUSSION

The aim of the current study was to develop an  $^{18}\text{F}$ -labeled dopamine  $D_2/D_3$  receptor agonist radioligand. For this purpose,  $^{18}\text{F}$ -MCL-524 was selected for radiolabeling on the basis of affinity in vitro to the  $D_2^{\text{high}}$  receptor. PET studies on monkeys demonstrated that  $^{18}\text{F}$ -MCL-524 provides a binding signal that is similar to, or even higher than, the previously developed radioligand  $^{11}\text{C}$ -MNPA. Blocking studies and preliminary kinetic analysis further supported the suitability of the radioligand properties of  $^{18}\text{F}$ -MCL-524. The longer half-life of  $^{18}\text{F}$  than of  $^{11}\text{C}$  is a unique property of  $^{18}\text{F}$ -MCL-524 in comparison to the already available  $^{11}\text{C}$ -labeled agonist radioligands.  $^{18}\text{F}$ -MCL-524 is thus an interesting candidate

**TABLE 2**  
Kinetic Rate Constants and  $V_T$ s of  $^{18}\text{F}$ -MCL-524

Region	Subject	1TCM					2TCM			GA	
		$K_1$ ( $\text{mL}\cdot\text{cm}^{-3}\cdot\text{min}^{-1}$ )	$k_2$ ( $\text{min}^{-1}$ )	SSR	AIC	$V_T$ ( $\text{mL}\cdot\text{cm}^{-3}$ )	SSR	AIC	$V_T$ ( $\text{mL}\cdot\text{cm}^{-3}$ )	$V_T$ ( $\text{mL}\cdot\text{cm}^{-3}$ )	
Striatum	M1	0.26 (0.9)	0.015 (2.0)	791	-14	17.1 (1.6)	793	-9	17.2 (2.4)	15.8 (0.23)	
	M2	0.30 (1.7)	0.020 (3.2)	1,388	24	14.9 (2.3)	1,369	29	14.9 (3.1)	14.7 (0.29)	
	M3	0.22 (1.4)	0.012 (3.1)	460	8	17.4 (2.3)	474	14	17.4 (2.5)	15.6 (0.38)	
	Mean	0.26 (1.3)	0.016 (2.7)	880	6	16.5 (2.0)	879	11	16.5 (2.7)	15.4 (0.30)	
Cerebellum	M1	0.21 (0.9)	0.044 (1.8)	247	-11	4.8 (1.3)	239	-7	NA	4.8 (0.40)	
	M2	0.29 (1.9)	0.067 (4.6)	1,490	63	4.4 (4.4)	1,501	68	4.3 (4.4)	4.7 (0.70)	
	M3	0.23 (0.7)	0.039 (1.4)	89	-18	5.8 (1.2)	89	-13	5.8 (2.2)	5.6 (0.29)	
	Mean	0.24 (1.2)	0.050 (2.6)	609	11	5.0 (2.3)	610	16	5.0 (3.3)	5.0 (0.46)	

SSR = sum of squared residuals; AIC = Akaike information criterion; NA = not available (2TCM could not calculate reasonable  $V_T$ ). SE coefficients of variation are presented between parentheses.



**TABLE 3**  
 $BP_{ND}$  Values of  $^{18}\text{F}$ -MCL-524 Calculated with MRTM, 1TCM, and GA

Region	M1			M2			M3			Mean		
	MRTM	1TCM	GA	MRTM	1TCM	GA	MRTM	1TCM	GA	MRTM	1TCM	GA
Striatum	2.3	2.6	2.3	2.1	2.4	2.1	1.7	2.0	1.8	2.0	2.3	2.1
Putamen	2.4	2.7	2.4	2.2	2.6	2.2	1.7	2.0	1.8	2.1	2.4	2.2
Caudate nucleus	2.1	2.4	2.2	1.9	2.2	2.0	1.8	2.2	1.9	2.0	2.3	2.0
Ventral striatum	1.6	1.7	1.5	1.5	1.8	1.5	1.4	1.6	1.4	1.5	1.7	1.5

for future PET studies on dopamine modulation in preclinical or clinical settings.

$^{18}\text{F}$  was introduced into the 2-position moiety of the aporphine scaffold. This approach is preferable to introduction of  $^{18}\text{F}$  into the *N*-alkyl chain, because the latter has been shown to be detrimental for the affinity in vivo to the  $D_2/D_3$  receptor (12).

Like the reference  $^{11}\text{C}$ -labeled ligand MNPA ( $5.1 \pm 1.3$  nM), MCL-524 has nanomolar ( $3.7 \pm 1.2$  nM) affinity to the  $D_2^{\text{high}}$  receptor in vitro (15). A direct comparison between the 2 radioligands in 3 cynomolgus monkeys demonstrated that  $^{18}\text{F}$ -MCL-524 provides similar or even higher contrast between the striatum and the cerebellum.

The favorable comparison with  $^{11}\text{C}$ -MNPA prompted a preliminary characterization of the specificity of binding. After administration of the selective reference  $D_2/D_3$  receptor antagonist raclopride, the binding of  $^{18}\text{F}$ -MCL-524 was markedly reduced (89% of striatal  $BP_{ND}$  values) to a degree similar to that previously reported for  $^{11}\text{C}$ -MNPA (5). This observation supports the view that  $^{18}\text{F}$ -MCL-524 binds specifically to  $D_2/D_3$  receptors in vivo. Administration of *D*-amphetamine reduced the striatal  $^{18}\text{F}$ -MCL-524 binding by 56%, similar to that previously reported for  $^{11}\text{C}$ -MNPA (27), supporting the view that  $^{18}\text{F}$ -MCL-524 has agonistic properties.

$^{18}\text{F}$ -MCL-524 underwent a moderate rate of metabolism, and the parent fraction in plasma was about 23% at 30 min after injection, which is similar to that reported for  $^{11}\text{C}$ -MNPA (28) and  $^{11}\text{C}$ -NPA (29). The observed radiometabolite fractions (Fig. 4A) eluted earlier from the reversed-phase column than  $^{18}\text{F}$ -MCL-524, suggesting that the radiometabolites are more polar and therefore less likely to pass the blood–brain barrier. The mean  $f_p$  of  $^{18}\text{F}$ -MCL-524 was 0.07, which is sufficiently large to allow for reliable quantification of plasma protein binding in applied studies.

A radiometabolite-corrected arterial input function was obtained in 3 monkeys examined with  $^{18}\text{F}$ -MCL-524. The obtained regional time–activity curves were evaluated using the 1TCM and 2TCM. It was anticipated that the cerebellum (negligible  $D_2/D_3$  receptor density) and striatum (high  $D_2/D_3$  receptor density) could be best described with the 1TCM and 2TCM, respectively. However, both regions could be described with the 1TCM, and the 2TCM was not statistically preferred. This observation is similar to that previously reported for  $^{11}\text{C}$ -NPA (29) and may indicate that the 4 rate constants of the 2TCM share sufficient similarities to allow for the curves to be described by the 2 rate constants of the 1TCM.

$BP_{ND}$  values were calculated with the MRTM but were also estimated using GA and the tissue compartment models.  $BP_{ND}$  values calculated with MRTM compared well with values of GA and the 1TCM, but the approximately 12%–14% underestimation by MRTM in comparison to the 1TCM may require further evaluation in human subjects.  $BP_{ND}$  values were stable after 60 or 90 min using the MRTM or 1TCM, respectively. Altogether, and considering reference tissue model advantages such as the redundancy of arterial cannulation and lower variability, a reference region approach such as the MRTM may be appropriate for clinical studies.

$^{18}\text{F}$ -MCL-524 provided striatal  $BP_{ND}$  values that were approximately 50% higher than those for  $^{11}\text{C}$ -MNPA. The relative ratio of  $^{18}\text{F}$ -MCL-524/ $^{11}\text{C}$ -MNPA was similar across striatal subregions. When the higher fraction of  $D_3$  receptors in the ventral striatum is considered, the similarity across subregions suggests that the radioligands have similar  $D_2$ -versus- $D_3$  receptor selectivity.

To prepare for human studies, we performed whole-body dosimetry on monkeys to estimate the radiation exposure in humans.

Similar to reports for  $^{11}\text{C}$ -MNPA and  $^{11}\text{C}$ -NPA (28,30), the organ with the highest uptake was the gallbladder. The extrapolated effective dose of  $^{18}\text{F}$ -MCL-524 (0.035 mSv/MBq) was comparable to other  $^{18}\text{F}$ -labeled radioligands, such as  $^{18}\text{F}$ -A-85380 (0.019–0.039 mSv/MBq) and  $^{18}\text{F}$ -SPA-RQ (0.032 mSv/MBq) (31). Moreover, it should be noted that dosimetry studies in monkeys may overestimate effective dose (32).

## CONCLUSION

We identified  $^{18}\text{F}$ -MCL-524 as a suitable radioligand for quantitative studies of  $D_2/D_3$  receptors in the monkey brain. The results warrant further evaluation of  $^{18}\text{F}$ -MCL-524

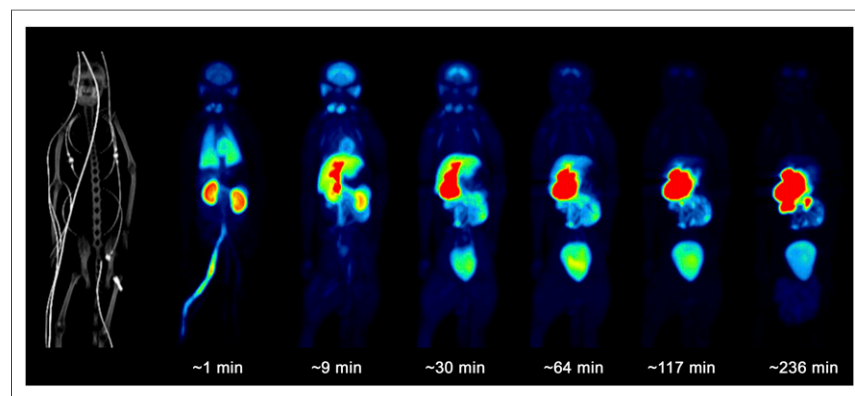


**FIGURE 5.** Whole-body PET/CT maximum-intensity-projection images after  $^{18}\text{F}$ -MCL-524 administration.

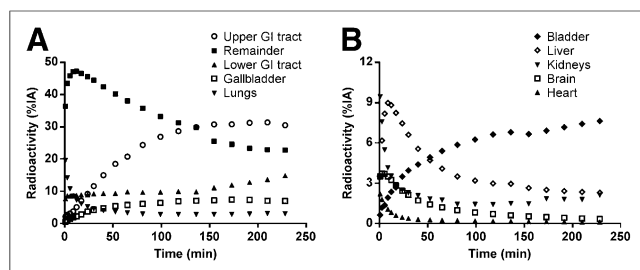


**FIGURE 6.** Time-activity course for  $^{18}\text{F}$ -MCL-524 in different organs and remainder of body. GI = gastrointestinal; %IA = percentage injected activity.

in human studies in preparation for applied clinical studies on changes in striatal dopamine concentration. The longer half-life of  $^{18}\text{F}$  makes  $^{18}\text{F}$ -MCL-524 particularly attractive for future application in bimodal PET/functional MRI for simultaneous measurement of changes in dopamine concentration and blood-oxygen-level-dependent signal.

## DISCLOSURE

The costs of publication of this article were defrayed in part by the payment of page charges. Therefore, and solely to indicate this fact, this article is hereby marked "advertisement" in accordance with 18 USC section 1734. Financial support was received

**TABLE 4**  
Radiation Dose Estimates of  $^{18}\text{F}$ -MCL-524 for Different Organs

Organ	Estimated dose (mSv/MBq)		
	M4	M5	Mean
Gallbladder wall	0.233	0.300	0.267
ULI wall	0.166	0.216	0.191
Small intestine	0.146	0.189	0.168
Thyroid	0.033	0.140	0.086
Urinary bladder wall	0.072	0.093	0.082
LLI wall	0.057	0.071	0.064
Kidneys	0.034	0.055	0.044
Ovaries	0.031	0.036	0.034
Uterus	0.027	0.031	0.029
Liver	0.020	0.025	0.022
Lungs	0.025	0.017	0.021
Stomach wall	0.014	0.014	0.014
Pancreas	0.014	0.014	0.014
Spleen	0.012	0.011	0.011
Red marrow	0.011	0.011	0.011
Adrenals	0.011	0.010	0.011
Heart wall	0.010	0.010	0.010
Osteogenic cells	0.011	0.008	0.009
Muscle	0.009	0.009	0.009
Testes	0.007	0.006	0.007
Brain	0.006	0.006	0.006
Thymus	0.007	0.004	0.005
Skin	0.006	0.004	0.005
Breasts	0.006	0.004	0.005
Total body	0.012	0.012	0.012
Effective dose	0.031	0.040	0.035

ULI = upper large intestine; LLI = lower large intestine.

from the Branfman Family Foundation and T32-DA007252. No other potential conflict of interest relevant to this article was reported.

## ACKNOWLEDGMENTS

We thank the members of the PET group at Karolinska Institutet for excellent assistance and in particular Gudrun Nylén for assistance in the PET studies.

## REFERENCES

- De Lean A, Kilpatrick BF, Caron MG. Dopamine receptor of the porcine anterior pituitary gland: evidence for two affinity states discriminated by both agonists and antagonists. *Mol Pharmacol*. 1982;22:290–297.
- George SR, Watanabe M, Di Paolo T, Falardeau P, Labrie F, Seeman P. The functional state of the dopamine receptor in the anterior pituitary is in the high affinity form. *Endocrinology*. 1985;117:690–697.
- Kühl M, Finnemann S, Binder O, Wedlich D. Dominant negative expression of a cytoplasmically deleted mutant of XB/U-cadherin disturbs mesoderm migration during gastrulation in *Xenopus laevis*. *Mech Dev*. 1996;54:71–82.
- Hwang DR, Kegeles LS, Laruelle M. (–)-N-[ $^{11}\text{C}$ ]propyl-norapomorphine: a positron-labeled dopamine agonist for PET imaging of  $\text{D}_2$  receptors. *Nucl Med Biol*. 2000;27:533–539.
- Finnema SJ, Seneca N, Farde L, et al. A preliminary PET evaluation of the new dopamine  $\text{D}_2$  receptor agonist [ $^{11}\text{C}$ ]MNPA in cynomolgus monkey. *Nucl Med Biol*. 2005;32:353–360.
- Wilson AA, McCormick P, Kapur S, et al. Radiosynthesis and evaluation of [ $^{11}\text{C}$ ](+)-4-propyl-3,4,4a,5,6,10b-hexahydro-2H-naphtho[1,2-b][1,4]oxazin-9-ol as a potential radiotracer for in vivo imaging of the dopamine  $\text{D}_2$  high-affinity state with positron emission tomography. *J Med Chem*. 2005;48:4153–4160.
- Narendran R, Hwang DR, Slifstein M, et al. In vivo vulnerability to competition by endogenous dopamine: comparison of the  $\text{D}_2$  receptor agonist radiotracer (–)-N-[ $^{11}\text{C}$ ]propyl-norapomorphine ([C-11]NPA) with the  $\text{D}_2$  receptor antagonist radiotracer [C-11]-raclopride. *Synapse*. 2004;52:188–208.
- Narendran R, Mason NS, Laymon CM, et al. A comparative evaluation of the dopamine  $\text{D}_{2/3}$  agonist radiotracer [ $^{11}\text{C}$ ](–)-N-propyl-norapomorphine and antagonist [ $^{11}\text{C}$ ]raclopride to measure amphetamine-induced dopamine release in the human striatum. *J Pharmacol Exp Ther*. 2010;333:533–539.
- Judenhofer MS, Wehr HF, Newport DF, et al. Simultaneous PET-MRI: a new approach for functional and morphological imaging. *Nat Med*. 2008;14:459–465.
- Laruelle M. Imaging synaptic neurotransmission with in vivo binding competition techniques: a critical review. *J Cereb Blood Flow Metab*. 2000;20:423–451.
- Finnema SJ, Bang-Andersen B, Wikström HV, Halldin C. Current state of agonist radioligands for imaging of brain dopamine  $\text{D}_2/\text{D}_3$  receptors in vivo with positron emission tomography. *Curr Top Med Chem*. 2010;10:1477–1498.
- Zijlstra S, Visser GM, Korf J, Vaalburg W. Synthesis and in vivo distribution in the rat of several fluorine-18 labeled N-fluoroalkylaporphines. *Appl Radiat Isot*. 1993;44:651–658.
- Vasdev N, Seeman P, Garcia A, et al. Syntheses and in vitro evaluation of fluorinated naphthoxazines as dopamine  $\text{D}_2/\text{D}_3$  receptor agonists: radiosynthesis, ex vivo biodistribution and autoradiography of [ $^{18}\text{F}$ ]F-PHNO. *Nucl Med Biol*. 2007;34:195–203.
- Shi B, Narayanan TK, Christian BT, Chattopadhyay S, Mukherjee J. Synthesis and biological evaluation of the binding of dopamine  $\text{D}_2/\text{D}_3$  receptor agonist, (R,S)-5-hydroxy-2-(N-propyl-N-(5'- $^{18}\text{F}$ -fluoropentyl)aminotetralin ( $^{18}\text{F}$ -5-OH-FPPAT) in rodents and nonhuman primates. *Nucl Med Biol*. 2004;31:303–311.
- Sromek AW, Si YG, Zhang T, George SR, Seeman P, Neumeyer JL. Synthesis and biological evaluation of N-fluoroalkyl and 2-fluoroalkoxy substituted aporphines: potential PET ligands for dopamine  $\text{D}_2$  receptors. *ACS Med Chem Lett*. 2011;2:189–194.
- Steiger C, Finnema SJ, Raus L, et al. A two-step one-pot radiosynthesis of the potent dopamine  $\text{D}_2/\text{D}_3$  agonist PET radioligand [ $^{11}\text{C}$ ]MNPA. *J Labelled Comp Radiopharm*. 2009;52:158–165.
- Garber JC, Barbee RW, Bielitzki JT, et al. *Guide for the Care and Use of Laboratory Animals*. 8th ed. Washington DC: National Academies Press; 2011:1–220.
- Finnema SJ, Stepanov V, Ettrup A, et al. Characterization of [C]Cimbi-36 as an agonist PET radioligand for the 5-HT and 5-HT receptors in the nonhuman primate brain. *Neuroimage*. 2014;84:342–353.

19. Varrone A, Stepanov V, Nakao R, et al. Imaging of the striatal and extrastriatal dopamine transporter with  $^{18}\text{F}$ -LBT-999: quantification, biodistribution, and radiation dosimetry in nonhuman primates. *J Nucl Med*. 2011;52:1313–1321.
20. Varrone A, Sjöholm N, Eriksson L, Gulyas B, Halldin C, Farde L. Advancement in PET quantification using 3D-OP-OSEM point spread function reconstruction with the HRRT. *Eur J Nucl Med Mol Imaging*. 2009;36:1639–1650.
21. Ichise M, Liow JS, Lu JQ, et al. Linearized reference tissue parametric imaging methods: application to [ $^{11}\text{C}$ ]DASB positron emission tomography studies of the serotonin transporter in human brain. *J Cereb Blood Flow Metab*. 2003;23:1096–1112.
22. Logan J, Fowler JS, Volkow ND, et al. Graphical analysis of reversible radioligand binding from time-activity measurements applied to [ $^{11}\text{C}$ -methyl]-(-)-cocaine PET studies in human subjects. *J Cereb Blood Flow Metab*. 1990;10:740–747.
23. Innis RB, Cunningham VJ, Delforge J, et al. Consensus nomenclature for in vivo imaging of reversibly binding radioligands. *J Cereb Blood Flow Metab*. 2007;27:1533–1539.
24. Foster D, Barrett P. Developing and testing integrated multicompartment models to describe a single-input multi-output study using the SAAM II software system. *Mathematical Modeling in Experimental Nutrition*. New York, NY: Springer; 1998:59–78.
25. Stabin MG, Siegel JA. Physical models and dose factors for use in internal dose assessment. *Health Phys*. 2003;85:294–310.
26. Stabin MG, Sparks RB, Crowe E. OLINDA/EXM: the second-generation personal computer software for internal dose assessment in nuclear medicine. *J Nucl Med*. 2005;46:1023–1027.
27. Seneca N, Finnema SJ, Farde L, et al. Effect of amphetamine on dopamine D2 receptor binding in nonhuman primate brain: a comparison of the agonist radioligand [ $^{11}\text{C}$ ]MNPA and antagonist [ $^{11}\text{C}$ ]raclopride. *Synapse*. 2006;59:260–269.
28. Seneca N, Skinbjerg M, Zoghbi SS, et al. Kinetic brain analysis and whole-body imaging in monkey of [ $^{11}\text{C}$ ]MNPA: a dopamine agonist radioligand. *Synapse*. 2008;62:700–709.
29. Hwang DR, Narendran R, Huang Y, et al. Quantitative analysis of (-)-N- $^{11}\text{C}$ -propyl-norapomorphine in vivo binding in nonhuman primates. *J Nucl Med*. 2004;45:338–346.
30. Laymon CM, Mason NS, Frankle WG, et al. Human biodistribution and dosimetry of the D2/3 agonist  $^{11}\text{C}$ -N-propylnorapomorphine ( $^{11}\text{C}$ -NPA) determined from PET. *J Nucl Med*. 2009;50:814–817.
31. Zanotti-Fregonara P, Lammertsma AA, Innis RB. Suggested pathway to assess radiation safety of  $^{18}\text{F}$ -labeled PET tracers for first-in-human studies. *Eur J Nucl Med Mol Imaging*. 2013;40:1781–1783.
32. Zanotti-Fregonara P, Innis RB. Suggested pathway to assess radiation safety of  $^{11}\text{C}$ -labeled PET tracers for first-in-human studies. *Eur J Nucl Med Mol Imaging*. 2012;39:544–547.



The Journal of  
NUCLEAR MEDICINE

## **$^{18}\text{F}$ -MCL-524, an $^{18}\text{F}$ -Labeled Dopamine $\text{D}_2$ and $\text{D}_3$ Receptor Agonist Sensitive to Dopamine: A Preliminary PET Study**

Sjoerd J. Finnema, Vladimir Stepanov, Ryuji Nakao, Anna W. Sromek, Tangzhi Zhang, John L. Neumeyer, Susan R. George, Philip Seeman, Michael G. Stabin, Cathrine Jonsson, Lars Farde and Christer Halldin

*J Nucl Med.* 2014;55:1164-1170.

Published online: May 1, 2014.

Doi: 10.2967/jnumed.113.133876

---

This article and updated information are available at:

<http://jnm.snmjournals.org/content/55/7/1164>

---

Information about reproducing figures, tables, or other portions of this article can be found online at:

<http://jnm.snmjournals.org/site/misc/permission.xhtml>

Information about subscriptions to JNM can be found at:

<http://jnm.snmjournals.org/site/subscriptions/online.xhtml>

*The Journal of Nuclear Medicine* is published monthly.  
SNMMI | Society of Nuclear Medicine and Molecular Imaging  
1850 Samuel Morse Drive, Reston, VA 20190.  
(Print ISSN: 0161-5505, Online ISSN: 2159-662X)

© Copyright 2014 SNMMI; all rights reserved.